# Outer Hadron Calorimeter (HO) calibration

A. Smoron,[1] L. Apanasevich,[1] and M. Zielinski[2]
[1] *University of Illinois, Chicago, Illionois 60607*
[2] *University of Rochester, Rochester, New York 14627*
(Dated: May 8, 2006)

We present initial results of Outer Hadronic Calorimeter (HO) calibration at 4 different angles *eta* ($\eta$) using the test beam run in 2004. RMS and mean values are taken from the energy distributions at these angles. RMS is divided by mean and this ratio is plotted versus different $k$ values. The minimum of the graph is estimated. The $k$ value at the minimum corresponds to the optimum weight constant that needs to be applied to the energy detected by the outer calorimeter.

## I. INTRODUCTION

We study the Compact Muon Solenoid's (CMS's) noise before data taking starts in order to know what to expect and to be ready to conclude the correct physics laws from the actual events record. CMS and ATLAS are the two main detectors at Large Hadron Collider (LHC) currently build near Geneva, Switzerland. LHC soon will become the biggest accelerator ever build with the circumference of 27km and total collision energy of 14TeV. It will consists of three small detectors that are already running and the two large mentioned above. The first collision at CMS is scheduled for the summer of 2007. Starting from the most inner part, the CMS detector is build of a Tracker, whose purpose is to measure the trajectories of charged particles curved by the magnetic field. Next to the tracker is an Electromagnetic calorimeter (ECAL) responsible for detecting the electron-positron pair production events. Then there are four kinds of hadronic calorimeters that provide good segmentation, hermeticity, energy resolution and full angular coverage up to $\eta = 5$. They are responsible for detecting Hadrons such as protons, neutrons, pions or Kaons, which are strongly interacting particles that feel the force, which binds nuclei together. Hadronic showers starts to develop later and have longer longitudinal and lateral dimensions then electromagnetic ones, therefore, the Hadron Calorimeter (HCAL) is thicker than the ECAL and is located farther away from the center of collision. The Electromagnetic Calorimeter is surrounded by the Barrel Hadronic Calorimeter (HB), which covers the central pseudorapidity region up to $\eta = 1.3$. The two Endcap Hadron calorimeters (HE) cover the end regions up to $\eta = 3$ and two Forward Calorimeters (HF) extend the coverage up to $\eta = 5$. The HB and HE are located inside a 13 m long 4T solenoid magnet. Central shower containment is improved with an array of scintillators located outside the magnet and called Outer Hadronic Calorimeter (HO). Our study focus on this most outer hadron calorimeter. The last and largest part of the CMS is the muon detector system, which surrounds all the other parts. The detail cross-sectional view of CMS detector indicating various angles $\eta$ is shown below. (See Fig. 1).

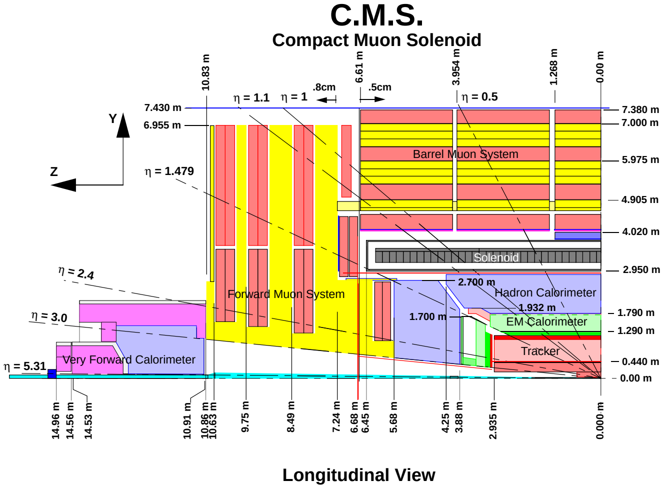

FIG. 1: An illustration of a two arm configuration in the $p_T$ plane (beam is oriented along the Z-axis). The lengths of the vectors represent their $p_T$. The angle between the two vectors is $\Delta\phi$. The projection of a $p_T$-vector onto the plane formed by the other vector and the beam axis yields $p_{OUT}$.

## II. HO STUDIES

### A. Details of the HO structure

Outer calorimeter was incorporated into CMS to improve the shower containment since as predicted about 5% of the energy of a $300 GeV$ pion would be deposited outside the HB calorimeter. HO consists of one or two layers of plastic scintillators with the same tower granularity as the HB, alternated by plates of brass. Outer hadron calorimeter is located beyond the solenoid and before the first muon layer. The *Ring* 0 region, the very central part of the detector is equipped with two layers of scintillators, while *Rings* 1 through 5 have only one furthermost HO scintillator layer available. The scintillators are read out through wavelength shifting optical fibres by photosensors in the barrel and endcap regions.

The photosensors are hybrid photodiodes, which consist of a fibre-optic entrance window onto which a photocathode is deposited, followed by a gap of several millimeters over which a large applied electric field accelerates photoelectrons onto a silicon diode target. The addition of the outer calorimeter extends the total depth of the calorimeter system from 5.8 $\lambda_I$ to 11.8 $\lambda_I$ and improves the energy resolution by 27% in 300 GeV pion resolution.

### B. Test Beam in 2004

The CMS HCAL has a permanent test beam facility in the CERN H2 beam, therefore, each year different sections of the calorimeter are tested using pion, electron and muon beams. A large motion table has been constructed on which two 20° wedges of HB, one 20° wedge of HE and one 40° wedge of HO, the length of a half barrel of HB, are placed. This table can move in $\eta$-$\phi$ to simulate the CMS detector. In order to test the HF calorimeter a special table was constructed for two 20° wedges, that can be moved up and down, sideways and tilted to fully simulate the detector in the test beam. All the movements are controlled by computers. The test beam has two different data acquisition (DAQ) systems; one for HF and the other one for HB, HE, and HO together. The test beam facility is also equipped with high and low voltage, slow control, moving radioactive source, laser and LED pulsing system. The test beam energy can vary from 25 to 100 GeV in case of electrons and from 25 to 300 GeV in case of pions, muons and protons. The beam can be used in a 2 second flat top or in one nsec bunches that are 25 nsec apart to simulate the LHC.

### C. Optimum weight constant $k$ from a test beam

From the principle of the conservation of energy we know that the initial energy of the accelerated particles just before the collision have to be equal to the sum of all energies recorded in different parts of the detector after the collision. Due to the electronic setup the part of the energy recorded by the Outer Hadron Calorimeter has to be multiplied by the weight constant. The weight constant corresponding to the energy part detected by the Barrel Calorimeter was for simplicity set to one. Therefore, the energy equation can be expressed by $E_{total} = E_b + kE_o$. In this equation $E_{total}$ represents the total energy of colliding particles, $E_b$ stands for the energy part recorded by the barrel calorimeter, $E_o$ is the energy part from the outer hadron calorimeter and $k$ represents the weight value that we are trying to estimate. The individual energy parts can be written as $E_i = G_i(N_i - N_i^*)$, where $G_i$ is a gain constant and $N$ is a number of ADC counts. As was mentioned before, our work was devoted to finding the optimum value of the $k$ constant using the test beam data recorded in 2004.

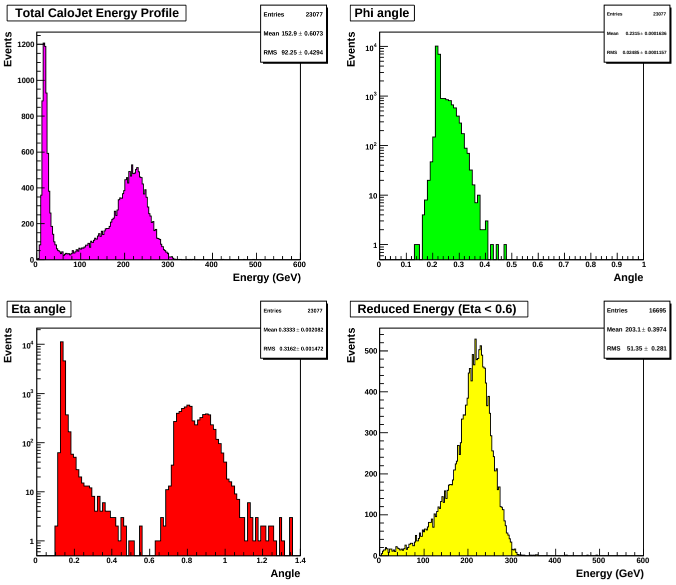

FIG. 2: The top left corner graph presents the energy profile detected during the test beam in 2004 at $\eta = 0.13$, $\phi = 0.22$ and $k = 6.8$. The top right corner figure shows the $\phi$ angles from which energy data was recorded. The bottom left graph shows the $\eta$ angles from which energy data was recorded, and the bottom right graph shows the energy profile after restricting the *eta* values to these smaller than 0.6

## III. RESULTS

### A. Events versus energy distribution

We have plotted the number of events versus the energy distributions recorded at four different angles $\eta$. Two of them very close to $\eta = 0$, one at $\eta = 0.55$, and one at the farthest possible test beam value of $\eta = 1.1$. Distributions at $\eta = 0.55$ and $\eta = 1.1$ were clearly Gaussian, but at $\eta$ close to zero we observed an additional events peak at energies very close to zero. As we found the second peak was a result of the leak of events recorded at $\eta$ approximately equal to 1. Therefore, we introduced cuts in the root macro written to plot these distributions restricting the value of angle $\eta$ to what we wanted. The example showing how the distribution profile looked before and after the cut is shown above (See Fig. 2). This profile corresponds to $\eta = 0.13$, $\phi = 0.22$ and $k = 6.8$. Clearly after the cut the distribution is Gaussian as we expected and it is possible to obtain the mean and RMS values from it.

### B. $k$ value results

From the events - energy distributions plotted using different $k$ values we obtained the corresponding mean and RMS values. Having these numbers we could divide

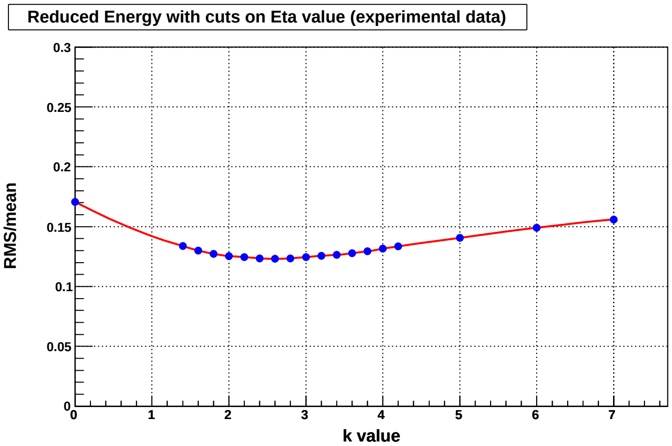

FIG. 3: A graph showing the dependence of the $RMS/mean$ values versus different $k's$ for the test beam data taken at $\eta = 0.55$ and $\phi = 0.22$. At this angle $\eta$ the cut in energy was not needed, therefore this is the most accurate representation we were able to obtain.

the RMS by mean and plot the obtained this way values versus the corresponding $k's$. As was predicted from the Monte-Carlo simulation these curves should have a clear minimum indicating the optimum value of $k$ at these particular angles $\eta$ and $\phi$. In our case, however, these minima's are not that evident. At $\eta = 0.55$ there is a clear minimum corresponding to $k = 2.6$, but the curvature of the graph is very shallow (See Fig. 3). At smaller $\eta$ values it is even worse and the plot for $\eta = 0.13$ shows almost a straight lines (See Fig. 4). That would mean that the $HO$ detector can not be calibrated, which is almost impossible. (Fig. 5) shows the calibration curve for $\eta = 1.1$, and (Fig. 6) for $\eta = 0.05$. As can be seen, none of these plots indicate an obvious optimum value calibration constant $k$. Looking at these graphs we might start to believe that $k$ should be somewhere between 3.5 and 4. These numbers, however, are unreasonably large. We want to point out that the sudden jump at $k = 4.6$ in (Fig. 5) and then the graduate drop is most likely an effect of the non-existing jet created by trying to use too high weight constants $k$. These numbers should not be that large, but for the purpose of our calculations we decided to used them just to see how the curve will behave. We also used them to see if we can find the minimum of the function, since we failed to do that with more reasonable values.

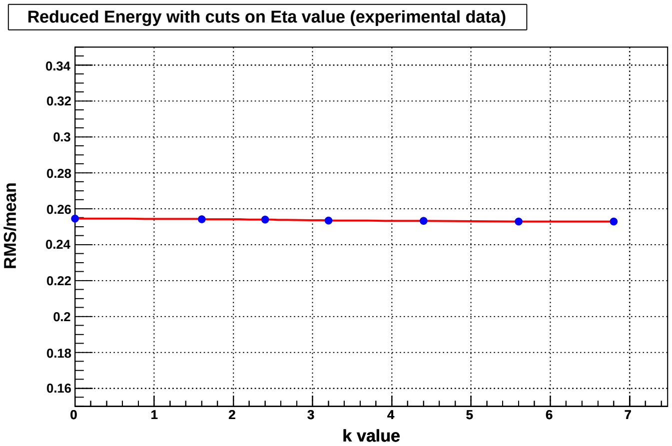

FIG. 4: A graph showing the dependence of the $RMS/mean$ values versus different $k's$ for the test beam data taken at $\eta = 0.13$, and $\phi = 0.22$

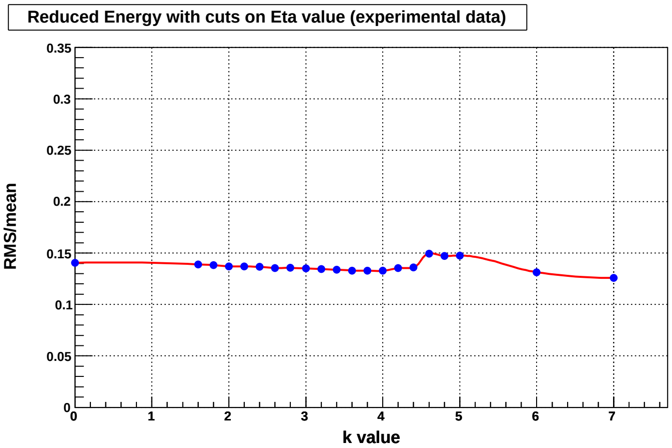

FIG. 5: A graph showing the dependence of the $RMS/mean$ values versus different $k's$ for the test beam data taken at $\eta = 1.1$, and $\phi = 0.22$. The sudden jump at $\eta = 4.6$ and the following graduate drop is most likely a result of the non-existing jet created by using too high $k$ values.

## IV. CONCLUSIONS

At this point we are not able to really conclude anything about the actual weight values $k$. We can only suspect that the optimum value at $\eta = 0.55$ is somewhere around $k = 2.6$, but even this number is not certain. We believe that for the failure that we experience might be responsible the software used CMSSW_0_3_0, which was not finalized and have many imperfections. Therefore, our immediate goal is to start utilizing the new version CMSSW_0_6_0, which was just released. We are hoping that this new improved version will allow us to figure out the true optimum $k$ values for all $\eta$ and $\phi$ angles.

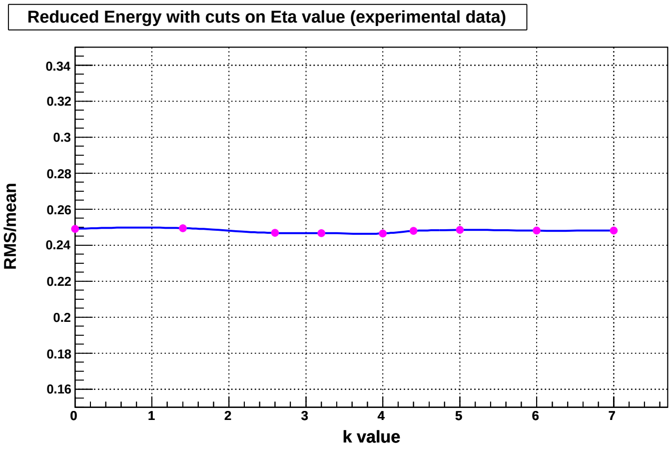

FIG. 6: A graph showing the dependence of the $RMS/mean$ values versus different $k's$ for the test beam data taken at $\eta = 0.05$, and $\phi = 2.2$. There is a possible minimum around $\eta = 3.5$.